Conf-911106--92

LBL-31457

Lawrence Berkeley Laboratory

UNIVERSITY OF CALIFORNIA

OSTI

MAR 2 4 1992

Presented at the IEEE Nuclear Science Symposium,
Santa FE, NM, November 5–9, 1991, and to
be published in the Proceedings

Monte Carlo Optimization of Depth-of-Interaction Resolution in PET Crystals

T.A. DeVol, W.W. Moses, and S.E. Derenzo

November 1991

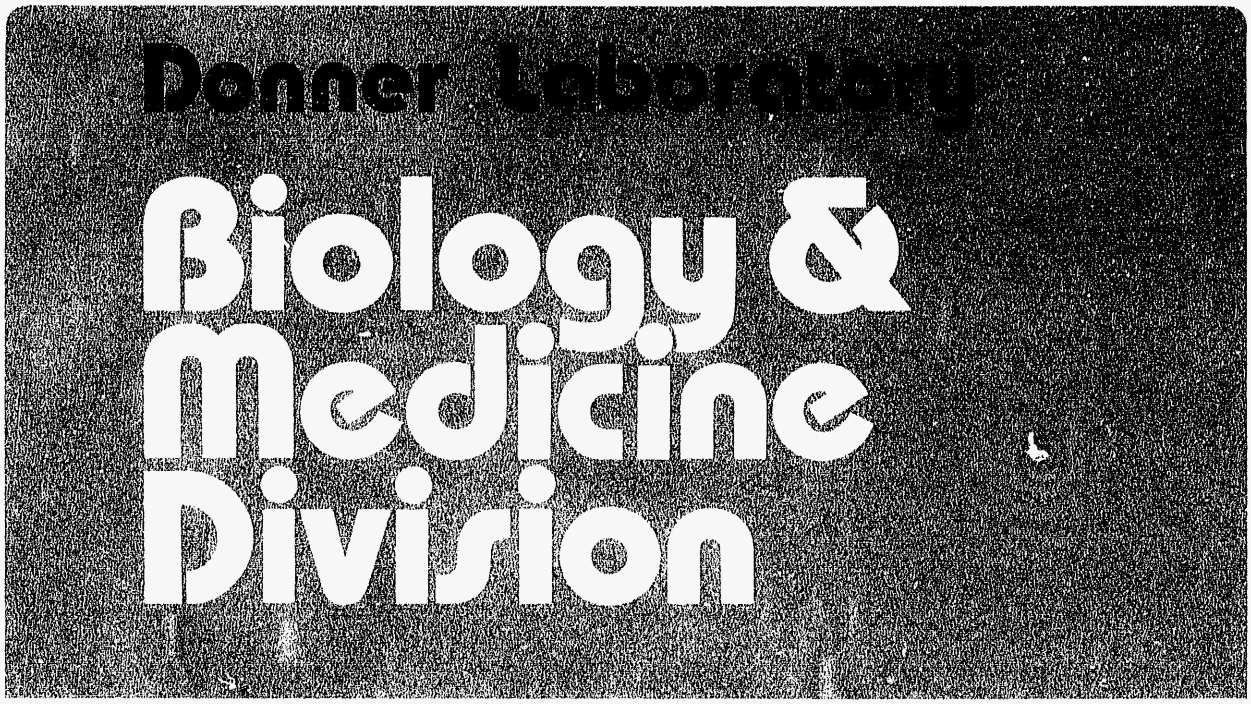

Prepared for the U.S. Department of Energy under Contract Number DE-AC03-76SF00098

DISTRIBUTION OF THIS DOCUMENT IS UNLIMITED

DISCLAIMER

This document was prepared as an account of work sponsored by the United States Government. Neither the United States Government nor any agency thereof, nor The Regents of the University of California, nor any of their employees, makes any warranty, express or implied, or assumes any legal liability or responsibility for the accuracy, completeness, or usefulness of any information, apparatus, product, or process disclosed, or represents that its use would not infringe privately owned rights. Reference herein to any specific commercial product, process, or service by its trade name, trademark, manufacturer, or otherwise, does not necessarily constitute or imply its endorsement, recommendation, or favoring by the United States Government or any agency thereof, or The Regents of the University of California. The views and opinions of authors expressed herein do not necessarily state or reflect those of the United States Government or any agency thereof or The Regents of the University of California and shall not be used for advertising or product endorsement purposes.

Lawrence Berkeley Laboratory is an equal opportunity employer.

LBL--31457

DE92 011147

Monte Carlo Optimization of Depth-of-Interaction Resolution in PET Crystals

T.A. DeVol

Department of Nuclear Engineering
University of Michigan
Ann Arbor, MI 48109-2100

and

W.W. Moses and S.E. Derenzo

Research Medicine and Radiation Biophysics Division
Lawrence Berkeley Laboratory
University of California
Berkeley, California 94720

November 1991

This work was supported in part by the Whitaker Foundation, by the National Institutes of Health, National Heart, Lung and Blood Institute and National Cancer Institute under Grant Nos. P01-HL25840 and R01-CA48002, and by the Director, Office of Energy Research, Office of Health and Environmental Research, Medical Applications and Biophysical Division, of the U.S. Department of Energy under Contract No. DE-AC03-76SF00098.

MASTER

DISTRIBUTION OF THIS DOCUMENT IS UNLIMITED

MONTE CARLO OPTIMIZATION OF DEPTH-OF-INTERACTION RESOLUTION IN PET CRYSTALS

T.A. DeVol[§], W.W. Moses[†], and S.E. Derenzo[†],
[§]Department of Nuclear Engineering, The University of Michigan, Ann Arbor, MI 48109-2100
and [†]Lawrence Berkeley Laboratory, University of California, Berkeley, CA. 94720

Abstract

The light distribution along one edge of a PET scintillation crystal was investigated with a Monte Carlo simulation. This position-dependent light can be used to measure the 511 keV photon interaction position in the crystal on an event by event basis, thus reducing radial elongation. The expected full width at half maximum (FWHM) of the light distribution on the 3 x 30 mm^2 surface of a 3 x 10 x 30 mm^3 bismuth germanate (BGO) crystal surrounded by a diffuse reflector was determined to be 3.0 mm. This light distribution does not change as the width (originally 3 mm) is varied from 1 to 6 mm, but decreases monotonically from 3.0 to 1.8 mm FWHM as the height (originally 10 mm) is reduced to 3 mm. Other geometrical modifications were simulated, including numerous corner reflectors on the opposing 3 x 30 mm^2 surface, which reduced the FWHM to 2.4 mm. The response of a dual wedge photodiode combined with the predicted light distribution for the 3 x 10 x 30 mm^3 BGO scintillation crystal results in an expected depth of interaction resolution of 7.5 mm FWHM.

I. INTRODUCTION

This paper addresses how to alleviate radial elongation, a PET imaging artifact, by determining the depth of interaction of a 511 keV photon along the axis of a PET scintillation crystal. This artifact is due to 511 keV photons penetrating into adjacent crystals before undergoing an interaction. The reconstruction algorithm, having no interaction position information, assigns the interaction to the surface of the crystal closest to the patient, which is the most probable place for the interaction. This possible mispositioning results in images with a spatially variant point spread function (PSF), *i.e.* radial elongation. For example, the Donner 600 Crystal Tomograph has a circular PSF with a FWHM of 2.6 mm at the center of the ring which, at a radius of 10 cm, becomes an ellipse with 2.8 mm tangential x 4.8 mm radial FWHM [1].

The radial elongation distortion can be eliminated by measuring the photon depth-of-interaction in the scintillation crystal on an event by event basis and using this information in the reconstruction algorithm. While a number of methods have been proposed for performing this measurement [2], this paper investigates placing a position sensitive photodiode along the edge of the crystal, as shown in Figure 1. Experimentally a dual wedge position sensitive photodiode was utilized to measure a depth-of-interaction resolution of 11 mm FWHM for a 3 x 10 x 30 mm^3 BGO crystal [3]. However, simulations have shown that 5 mm FWHM depth-of-interaction resolution is needed to eliminate radial elongation [4].

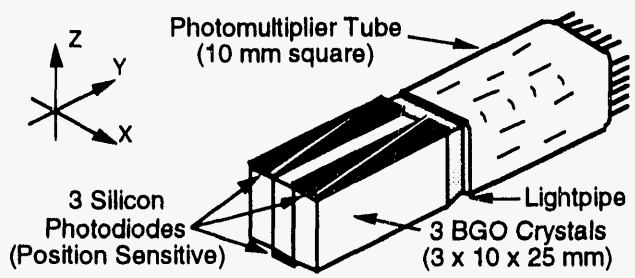

Figure 1: Detector Assembly

Monte Carlo simulations to determine the light distribution in a PET scintillation crystal are investigated. The purpose is to optimize the design of the detector module and achieve the requisite 5 mm FWHM depth-of-interaction resolution. Specific attention is paid to the distribution of scintillation light along the edge of the crystal which is coupled to the position sensitive detector (*i.e.* photodiode), as this distribution is the main factor that determines the depth-of-interaction resolution. This work is an extension of previous work by others that optimize either the total amount of light seen on one surface of the scintillation crystal [5,6] or the time distribution of the detected scintillation photons [7].

II. METHOD

A. *Monte Carlo Simulation*

The detection system modeled is that shown in Figure 1, with the exception that only one of the three scintillation

*This work was supported in part by the U. S. Department of Energy under contract No. DE-AC03-76SF00098, in part by Public Health Service Grants No. PO1 25840 and R01 CA48002, and in part by a grant from the Whitaker Foundation.

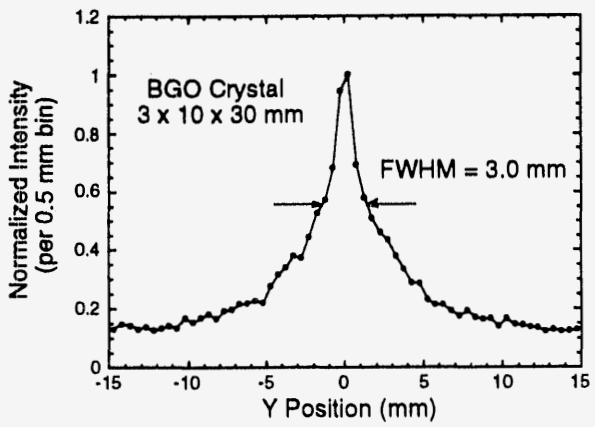

Figure 2: Typical Light Distribution

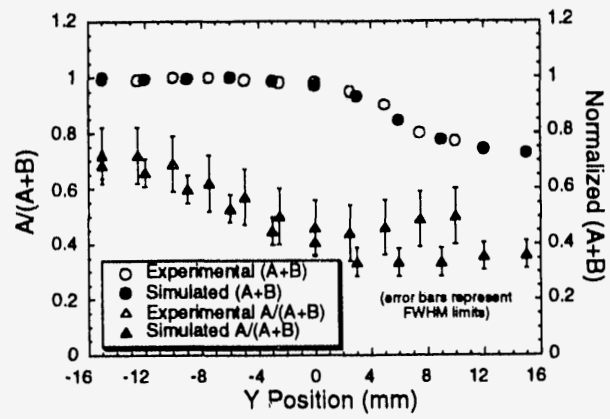

Figure 3: Comparison of Experiment and Simulation

crystal / photodiode assemblies is simulated. A timing signal from a 511 keV photon interaction is generated from the photomultiplier tube (PMT) that is coupled to a X-Z surface of the crystal. The position sensitive photodiode (PD) coupled to a X-Y crystal surface serves two purposes: to identify the crystal of interaction and determine the axial position of that interaction. The photodetectors were modeled as having a quantum efficiency of 30% and 60%, and reflectivity of 40% [8] and 10% for the PMT and PD respectively. The BGO crystal was modeled as having a mean free path to scatter and absorption of 400 mm [9] and an index of refraction of 2.15. The crystal was assumed to have polished surfaces that were separated by a small air gap from a diffuse reflector with 98% reflectivity. Transparent optical coupling compound having a index of refraction of 1.5 was used to couple the photodetectors to the crystal.

The above data was used as input to DETECT [10], a Monte Carlo program developed to study light collection properties in scintillators. DETECT generates individual photons in a specified portion of the scintillating crystal, follows each photon in its passage through the various components and interactions with surfaces, models absorption, scatter, and absorption and re-emission by a wavelength shifting component, and records the fate (absorption, escape, or detection) of each photon. The program outputs the fraction of emitted photons that are detected by both the PMT and the PD, as well as the Y coordinate of the photons detected by the position sensitive PD.

Incoming 511 keV photons were assumed to interact at a fixed depth (*i.e.* Y coordinate), and so the luminescent center was defined to be an X-Z plane centered at a given Y position. Figure 2 shows a typical light distribution (in 0.5 mm bins) along the 3 x 30 mm^2 edge of a 3 x 10 x 30 mm^3 BGO crystal excited at Y=0 mm.

In order to estimate the position resolution of the entire detector system, a second Monte Carlo simulation was performed. This simulation has as input a light distribution (similar that found in Figure 2), the effects of electronic noise in the photodiodes, Compton interactions in the BGO crystal, and the BGO light output (including statistical fluctuations) to predict how the photodiode signal varies as a function of the Y interaction position. The position sensitive photodiode was a dual wedge design, with wedges labeled "A" and "B." The interaction position was determined by computing the ratio of the signal measured by "A" to the total signal A+B, that is A/(A+B), which ideally would vary from 0 to 1.

B. *Experimental Verification*

To validate our simulation, the experimental configuration shown in Figure 1 [3] was modeled. This was a 3 x 10 x 30 mm^3 BGO crystal attached to a 20 mm long PD that was positioned between Y = -15 mm and Y = +5 mm, and a PMT at Y = +15 mm. Note that the photodiode covered only a portion of the scintillation crystal. The parameters used by the simulation were chosen to mimic the experimental conditions. The operating temperature was -100° C, so the BGO light output was set to 27,000 photons per MeV of deposited energy [11]. The electronic noise in each of the photodiode wedges was 275 electrons FWHM (determined by direct measurement), and the luminescent center size was smeared by 3 mm to simulate the experimentally determined spread of the electronically collimated beam of 511 keV photons (this includes the effects of Compton interactions in the BGO crystal).

Figure 3 shows the experimental and simulated values of A/(A+B) as a function of the Y position, where the error bars represent the FWHM of the A/(A+B) distribution at each position. The simulation correctly predicts the shape of curve (except for a small disagreement at positions greater than Y = +5 mm, where there is no PD coverage), but consistently underestimates the width of the A/(A+B) distribution. This is thought to be a fault of the electronic circuit that computes A/(A+B), and not the modeling. The position resolution is determined by dividing the width of the A/(A+B) distribution by the slope of the A/(A+B) vs. Y curve measured between -12 mm and

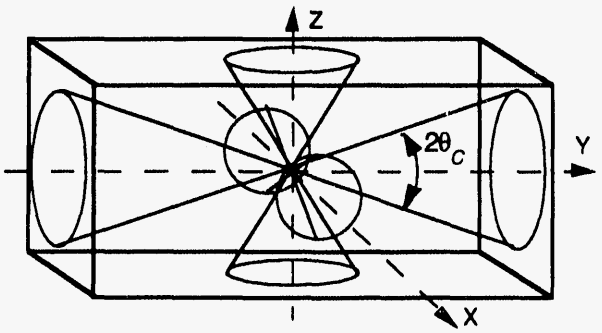

Figure 4: Light Cones as Defined by the Critical Angle

0 mm [3]. Doing this, the experimental position resolution is 11 mm FWHM, while the simulation predicts 5.8 mm FWHM.

III. Results and Discussion

A. *Theoretical Model*

While scintillation light emanates from its luminescent center isotropically into 4π, its distribution on a given surface of the scintillation crystal can be far from uniform; this non-uniformity is used to determine the position of the luminescent center. The degree of non-uniformity is determined by the geometric, optical, and surface properties of the crystal, reflector, and photodetectors. The primary focus of this paper is to investigate the properties that change the light distribution along the axis of a scintillation crystal, and optimize it for measuring the axial interaction position.

When light traveling in a medium with index of refraction n_2 impinges a medium with lower index of refraction n_1, it will undergo total internal reflection if its angle of incidence (with respect to the normal to the surface) is greater than the critical angle

$$sin(\theta_C) = n_1/n_2 \ , \tag{1}$$

which is 27.7° for BGO ($n = 2.15$) surrounded by air. This implies that only a fraction of the scintillation photons

$$\Omega_{cone} = 0.5(1 - cos(\theta_C)) \tag{2}$$

can directly illuminate any crystal surface [5], and these photons will only illuminate a portion of the surface, as illustrated by Figure 4.

In a perfect rectangular parallelepiped crystal, the light exiting a given surface (and entering a photodetector placed on that surface) can be classified into three components. The first is a "direct" component, comprised of photons that are inside the light cone and directed towards the detection surface. This "direct" light forms a narrow beam that lies within a circle defined by the critical angle that is centered above the luminescent center. This direct light can be detected by a position sensitive photodetector and determine the position of interaction. The rest of the light, $4\pi - \Omega_{cone}$, may eventually be detected by the photodetector, but must change direction at least once before doing so. This light is termed "diffuse," and has two origins. One origin is photons from the other 5 light cones that exit the crystal, are scattered by the diffuse reflector, and reenter the crystal in such a way as to be detected. The second diffuse component is comprised of photons that are initially outside the light cones, $4\pi - 6\Omega_{cone}$, and internally trapped, but scatter randomly from crystalline imperfections and are detected. The detection position of a "diffuse" photon is uncorrelated with the position of the luminescent center, and so these photons illuminate the photodiode uniformly.

The effects of the "direct" and "diffuse" components can be illustrated with Figure 2. The "direct" component forms the peak whereas the "diffuse" component forms the uniform background under the peak. The peak-to-background ratio and FWHM of the "direct" light distribution are the major factors that determine the depth-of-interaction resolution.

B. *Dependence on Crystal Size*

Varying the dimensions of the crystal can change the diameter of the circle containing the "direct" light, and thus affect the FWHM of the light distribution. It can also affect the total signal measured by the PMT and position sensitive PD, which must remain high to assure that the signal to noise is sufficient for proper signal processing. The PMT signal must be large enough to generate an accurate timing signal, as well as have sufficient pulse height resolution to reject photons that have Compton scattered. Electronic noise is a contributing factor to the PD signal, so the PD signal due to scintillation photons must be large enough to accurately measure the interaction position of the scintillation crystal. It is expected that the FWHM of the position dependent light would not vary with the crystal width (the X dimension), since the diameter of circle defined by the light cone geometry remains unchanged. Figure 5 shows that this is the case, with the FWHM of the light distribution fluctuating around 3.0 mm. Figure 5 also shows that the PMT and PD photon detection efficiencies are a constant 13% and 22% respectively.

Of greater interest is the dependence of these signals on the height (Z dimension) of the crystal. It is expected that as the height is decreased, the diameter of circle defined by the light cone at the detection surface would also decrease, reducing the FWHM of light distribution. Figure 6 shows that as the height is decreased from 10 mm to 3 mm, the light distribution decreases from 3.0 mm to 1.8 mm FWHM. The PMT and PD photon detection efficiencies are again a roughly constant 13% and 22% respectively. Therefore, the interaction position measurement resolution can be improved, without degrading the PMT performance, by reducing the height (Z dimension).

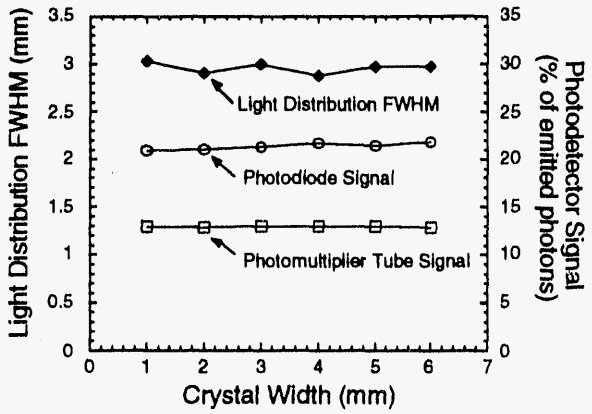

Figure 5: Light Distribution and Photodetector Signals as a Function of Crystal Width for a X mm x 10 mm x 30 mm BGO Crystal

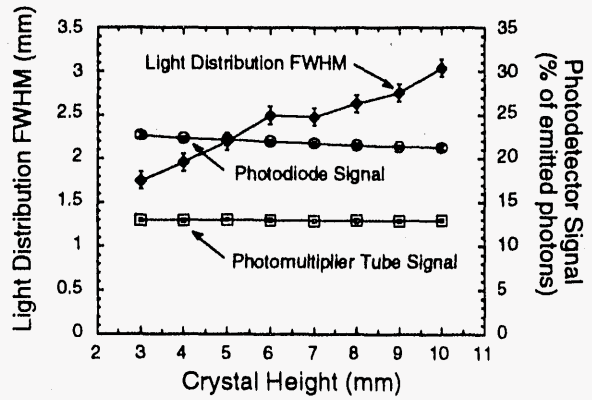

Figure 6: Light Distribution and Photodetector Signals as a Function of Crystal Height for a 3 mm x Z mm x 30 mm BGO Crystal

C. *Dependence on Surface Treatment*

In some situations, the crystal size is fixed by other constraints but improved position resolution is desired. For this reason, DETECT was used to investigate the effect of various surface treatments on the position dependent light. The first attempt was to decrease the "diffuse" light signal (while not affecting the "direct" component) by coupling a black reflector (0% reflectivity) directly to the crystal surface opposite the position sensitive PD. This reduced the FWHM of the light distribution to 2.1 mm for a 3 x 10 x 30 mm^3 BGO crystal, but also reduced the PMT and PD photon detection efficiencies to 2.5% and 7% respectively. Because of the electronic noise level in the PD, this loss in signal was shown experimentally to worsen the interaction position measurement resolution.

The previous example shows that the only way to improve the position resolution is to increase the "direct" light signal, hopefully by converting some of the "diffuse" light into "direct" light. This was attempted by modeling a crystal whose surface opposite the PD was cut to form numerous corner reflectors (Figure 7), causing photons that were in the light cone oriented away from the PD to undergo two total internal reflections and return oriented antiparallel to their initial direction. This almost doubles the "direct" component of the PD signal and decreases the FWHM of the light distribution to 2.4 mm in a 3 x 10 x 30 mm^3 BGO crystal. The photon detection efficiency of the PD is increased to 25%, but the PMT efficiency is reduced to 7%.

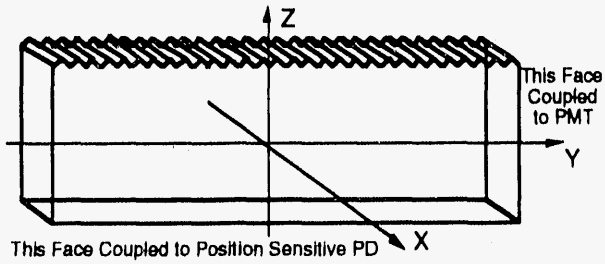

Figure 7: Crystal With Multiple Corner Reflectors

D. *Axial Position Resolution*

The radial PSF of the Donner 600 (which utilizies no depth-of-interaction information) is 4.8 mm FWHM, at a radius of 10 cm from the center of the tomograph ring [1]. This radial PSF can be reduced to 3.2 mm FWHM if the depth-of-interaction resolution is 5 mm FWHM, or 3.0 mm FWHM if the interaction position is exactly known [4]. Depth-of-interaction resolution was estimated for several of the above geometries using the method described in Section IIB, concentrating on the geometries with a depth-of-interaction resolution of 5 mm FWHM or better. Simulation results of a 3 x 30 mm^2 dual wedge position sensitive PD coupled to a 3 x 10 x 30 mm^3 BGO crystal with corner reflectors are shown in Figure 8. The A/(A+B) ratio and the FWHM of its distribution as well as the total PD signal are plotted at various luminescent center positions. The expected position resolution is 5 mm FWHM, compared to 7.5 mm FWHM for 3 x 10 x 30 mm^3 crystal without corner reflectors. This is mainly due to the smaller light distribution FWHM caused by the corner reflectors. Note that the 7.5 mm FWHM for the 3 x 10 x 30 mm^3 BGO crystal without corner reflectors is greater than the resolution predicted in Section IIB because the position is now measured over a 30 mm length rather than a 20 mm length.

The design of the proposed ultra-high resolution PET detector module was modified based on the data presented above. The crystal height is reduced from 10 mm to 5 mm and the width reduced from 3 mm to 2.2 mm. This results in each 1 cm square photomultiplier tube being coupled to eight 2.2 x 5 x 30 mm^3 BGO crystals rather than three 3 x 10 x 30 mm^3 crystals [3]. Figure 8 also shows the expected depth-of-interaction characteristics with this smaller crys-

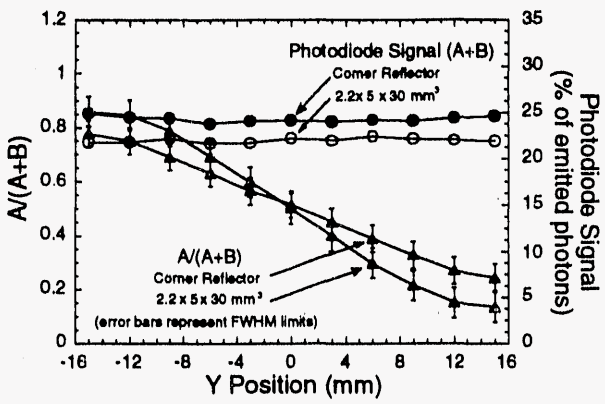

Figure 8: A/(A+B) and Photodiode Signal as a Function of Axial Position for the Corner Reflector Geometry and the 2.2 mm x 5 mm x 30 mm BGO Crystal

tal size. The light distribution FWHM is decreased to 2.2 mm, but the total PMT and PD signals are the same as with a 3 x 10 x 30 mm^3 crystal. The position resolution with a dual wedge photodiode is again estimated, and a depth-of-interaction resolution of 3 mm FWHM is predicted. This improvement is mainly due to the steeper slope of the A/(A+B) versus position curve.

IV. Conclusion

Simulations were performed of the light distribution along the edge of a PET scintillation crystal in order to optimize its ability to measure the 511 keV photon interaction axial position in that crystal. A 3 x 10 x 30 mm^3 BGO crystal surrounded by a diffuse reflector is predicted to yield a depth-of-interaction position resolution of 7.5 mm FWHM. This resolution is reduced to 3 mm at a crystal height of 5 mm, but is not affected by changing the width. The total amount of light detected on any surface is essentially unchanged by any of these modifications. Cutting numerous corner reflectors into the 3 x 30 mm^2 surface of a 3 x 10 x 30 mm^3 crystal will improve the position resolution to 5 mm FWHM, but will reduce the light on the 3 x 10 mm^2 surface by 50%. The multiple corner reflector and 2.2 x 5 x 30 mm^3 geometries both show promise as elements for an ultra-high resolution PET detector module designed to eliminate the radial elongation artifact.

Acknowledgements

This work was supported in part by the Director, Office of Energy Research, Office of Health and Environmental Research, Medical Applications and Biophysical Research Division of the U. S. Department of Energy under contract No. DE-AC03-76SF00098, in part by Grants No. PO1 25840 and R01 CA48002 awarded by the National Institutes of Health, National Heart, Lung, and Blood Institute and National Cancer Institute. One of us (T.A. DeVol) thanks the Environmental Restoration and Waste Management Fellowship Program, which is administered by Oak Ridge Associated Universities for the U.S. Department of Energy, for support, and one of us (W.W. Moses) thanks The Whitaker Foundation for support.

References

[1] S.E. Derenzo, R.H. Huesman, J.L. Cahoon, *et al.*, "A Positron Tomograph with 600 BGO Crystals and 2.6 mm Resolution," *IEEE Trans. Nuc. Sci.*, NS-35 (1988) 659-664.

[2] P. Bartzakos and C.J. Thompson, "A Depth-Encoded PET Detector," *IEEE Trans. Nucl. Sci.*, NS-38 (1991) 732-738.

[3] S.E. Derenzo, W.W. Moses, H.G. Jackson, *et al.*, "Initial Characterization of a Position-Sensitive Photodiode/BGO Detector for PET," *IEEE Trans. Nucl. Sci.*, NS-36, No. 1 (1989) 1084-1090.

[4] W.W. Moses, R.H. Huesman, and S.E. Derenzo, "A New Algorithm for using Depth-of-Interaction Measurement Information in PET Data Acquisition," *J. Nucl. Med.*, Vol. 32, No. 5 (1991) 995.

[5] W.A. Shurcliff and R.C. Jones, "The Trapping of Fluorescent Light Produced within Objects of High Geometrical Symmetry," *J. Opt. Soc. Am.*, Vol. 39, No. 11 (1949) 912-916.

[6] C. Carrier and R. LeComte, "Effects of Geometrical Modifications and Crystal Defects on the Light Collection in Ideal Rectangular Parallelepipedic BGO Scintillators," *Nucl. Instr. Meth.*, A294 (1990) 355-364.

[7] S.I. Ziegler, H. Ostertag, *et al.*, "Effects of Scintillation Light Collection on the Time Resolution of a Time-of-Flight Detector for Annihilation Quanta," *IEEE Trans. Nucl. Sci.*, NS-37 (1990) 574-579.

[8] W.D. Gunter, Jr., G.R. Grant, and S.A. Shaw, " Optical Devices to Increase Photocathode Quantum Efficiency," *Appl. Opt.*, Vol. 9, No. 2 (1970) 251-257.

[9] S.E. Derenzo and J.K. Riles, "Monte Carlo Calculation of the Optical Coupling Between Bismuth Germanate Crystals and Photomultiplier Tubes," *IEEE Trans. Nucl. Sci.*, NS-29, No. 1 (1982) 191-195.

[10] G.K. Knoll, T.F. Knoll, and T.M. Henderson, "Light Collection in Scintillation Detector Composites for Neutron Detection," *IEEE Trans. Nuc. Sci.*, NS-35, No. 1 (1988) 872-875.

[11] M.J. Weber and R.R. Monchamp, "Luminescence of $Bi_4Ge_3O_{12}$: Spectral and Decay Properties," J. Appl. Phys., Vol. 4 (1973) 5495-5499.

END

DATE FILMED

5/21/92